

large gap around  $z=0$  and  $z=c/2$  explains cleavage, the flakes being parallel to the (001) plane. The crossed packing of the molecules, apparent from the projection in Fig. 2, explains the positive optical sign of dibenzofuran. The bond angles in the five-membered rings vary from  $104.4$  to  $112.9^\circ$  with an average of  $108.5^\circ$  and those in the six-membered rings in the range  $115.3$  to  $123.9^\circ$  with an average of  $119.6^\circ$ . The individual six and five-membered rings are strictly planar but the whole molecule is not in a plane. In fact the molecule appears to have taken a slight 'boat' configuration, the benzene rings showing a dihedral angle of  $1.2^\circ$  with the furan ring. It is interesting that this result is similar to those observed in the cases of carbazole and dibenzoselenophene, molecules of nearly identical size and shape.

Table 9. *Some intermolecular distances*

C(1), I-C(3), II	3.99 Å	O(7), I-O(1), IV	3.83 Å
C(1), I-C(4), II	3.76	C(1), I-V(1), V	3.88
O(7), I-C(4), II, VIII	3.80	C(3), I-C(2), VI	3.96
C(2), I-C(2), III	3.98	C(4), I-C(2), VI	3.94
C(3), I-C(2), III	3.89	C(3), I-C(3), VII	3.98
O(7), I-C(4), IV, V	3.96	C(4), I-C(4), VII	3.85
O(7), I-C(5), IV, V	3.65	C(5), I-C(4), VII	3.77
O(7), I-C(6), IV, V	3.42	C(6), I-C(4), VII	3.74

## Positions:

I	$x, y, z$	V	$\frac{1}{2}+x, 1\frac{1}{2}-y, z$
II	$x, 1+y, z$	VI	$\frac{1}{2}-x, \frac{1}{2}-y, z$
III	$-x, 1-y, 1-z$	VII	$\frac{1}{2}+x, \frac{1}{2}-y, z$
IV	$\frac{1}{2}+x, 1\frac{1}{2}-y, \frac{1}{2}-z$	VIII	$x, 1+y, \frac{1}{2}-z$

The author expresses his deep sense of gratitude to Professor B. S. Basak for his able guidance and for providing all facilities. He is also thankful to the U.G.C. for financial assistance and the Tata Institute of Fundamental Research, Bombay for providing the CDC 3600 Computer facility.

## References

- BANERJEE, A. (1971). *Proc. Indian Sci. Cong.* **42** (III), 72.  
 BANERJEE, A. (1972). *Indian J. Phys.* **46**, 481-483.  
 BURNS, D. M. & IBALL, J. (1960). *Proc. Roy. Soc. A* **257**, 491.  
 BUSING, W. R., MARTIN, K. O. & LEVY, H. A. (1962). *ORFLS*. Report ORNL-TM-305, Oak Ridge National Laboratory, Oak Ridge, Tennessee.  
 CAMERMAN, A. & TROTTER, J. (1964). *Proc. Roy. Soc. A* **279**, 129.  
 COULSON, C. A. & GOLEBIEWSKI, A. (1961). *Proc. Phys. Soc.* **78**, 1310.  
 DEWAR, M. J. S., HARGET, A. J., TRINAJSTIC, N. & WORLEY, S. D. (1970). *Tetrahedron*. **26**, 4505-4516.  
 HOPE, H., KNOBLER, C. & MCCULLOUGH, J. D. (1970). *Acta Cryst.* **B26**, 628.  
 KAY, M. I., OKAYA, Y. & COX, O. E. (1971). *Acta Cryst.* **B27**, 26.  
 KURAHASHI, M., FUKUYO, M., SHIMADA, A., FURUSAKI, A., NITTA, I. (1968). *Bull. Chem. Soc. Japan*, **42**, 2174-2179.  
 LAHIRI, B. N. (1968). *Z. Kristallogr.* **127**, 456.  
 NISHIMOTO, K. & FORSTER, S. L. (1966). *Theor. Chim. Acta.* **4**, 155-165.  
 WILSON, A. J. C. (1949). *Acta Cryst.* **2**, 318-321.

*Acta Cryst.* (1973). **B29**, 2074

## Crystal Structure of $\text{La}_2(\text{MoO}_4)_3$ , a New Ordered Defect Scheelite Type

BY WOLFGANG JEITSCHKO

Central Research Department,\* E. I. du Pont de Nemours & Company, Experimental Station, Wilmington, Delaware 19898, U.S.A.

(Received 9 March 1973; accepted 14 May 1973)

$\text{La}_2(\text{MoO}_4)_3$  crystallizes with monoclinic symmetry, space group  $C2/c$ , and lattice constants  $a=17.006$  (4),  $b=11.952$  (2),  $c=16.093$  (3),  $\beta=108.44$  (3)°. Its crystal structure has been determined from single-crystal counter data and refined to a conventional  $R$  value of 0.055 for the 2031 structure factors greater than three standard deviations. The structure is related to the scheelite ( $\text{CaWO}_4$ ) structure from which it can be derived through vacancy ordering of  $\frac{1}{3}$  of the Ca sites. It comprises 9 scheelite subcells. There are 12 formula units per unit cell. Nearest-neighbor environments of the cations resemble those of scheelite: La is in eightfold and Mo in slightly distorted tetrahedral oxygen coordination. One third of the oxygen atoms are coordinated by one Mo and two La atoms, the other two thirds are coordinated by one Mo and one La atom. Interatomic distances reflect the differences in coordination. The structure is discussed and compared to the other known defect scheelite structures,  $\text{Eu}_2(\text{WO}_4)_3$  and  $\text{Bi}_2(\text{MoO}_4)_3$ .

### Introduction

The discovery of ferroelectricity (Borchardt & Bierstedt, 1966) and ferroelasticity (Aizu, 1969) in

$\text{Gd}_2(\text{MoO}_4)_3$  has stimulated extensive work in many laboratories and has led to thorough investigations of the rare-earth molybdates and tungstates with compositions  $\text{L}_2(\text{MoO}_4)_3$  and  $\text{L}_2(\text{WO}_4)_3$ , where L is a rare earth element. These compounds belong to at least five structural types: the  $\text{Eu}_2(\text{WO}_4)_3$  structure (Templeton

\* Contribution No. 2007.

& Zalkin, 1963); the  $\text{Sc}_2(\text{WO}_4)_3$  structure (Abrahams & Bernstein, 1966a); the prototypic and ferroic  $\text{Gd}_2(\text{MoO}_4)_3$  structures (Abrahams & Bernstein, 1966b; Jeitschko, 1970; Keve, Abrahams & Bernstein, 1971; Jeitschko, 1972) which collapse under high pressure forming an amorphous ( $\pi$ ) modification (Brixner, 1972); and the structure determined in the present paper. The occurrence of these types for  $\text{L}_2(\text{MoO}_4)_3$  compositions is summarized in Fig. 1. The structures of some phases occurring at high temperatures with some of the smaller rare earth metals are still not known (Nassau & Shiever, 1972; Brixner, 1972).

Both the  $\text{Eu}_2(\text{WO}_4)_3$  and the  $\text{La}_2(\text{MoO}_4)_3$  structures are derived from the  $\text{CaWO}_4$  (scheelite) structure (Silén & Nylander, 1943; Zalkin & Templeton, 1964; Kay, Frazer & Almodovar, 1964; Burbank, 1965). They can be represented by formulas  $\text{Eu}_{2/3}\square_{1/3}\text{WO}_4$  and  $\text{La}_{2/3}\square_{1/3}\text{MoO}_4$  where  $\square$  indicates vacant sites. The ordered arrangement of the vacancies gives rise to superstructures.

The present paper reports the crystal structure of  $\text{La}_2(\text{MoO}_4)_3$  which is also found for  $\text{Ce}_2(\text{MoO}_4)_3$ ,  $\alpha\text{-Pr}_2(\text{MoO}_4)_3$ , and  $\alpha\text{-Nd}_2(\text{MoO}_4)_3$  (Brixner, Sleight & Licis, 1972). A refinement of the scheelite-subcell of  $\alpha\text{-Nd}_2(\text{MoO}_4)_3$  has been published by Jamieson, Abrahams & Bernstein (1969). The unit cell for the full structure reported in that account was, however, not confirmed by Brixner, Sleight & Licis (1972) who gave cell dimensions for the four above-mentioned defect scheelites. The results reported by the latter authors are substantiated by the present structure determination.

### Experimental

Single crystals of  $\text{La}_2(\text{MoO}_4)_3$  can be grown by the Czochralski technique and presumably have a disordered defect-scheelite structure at high temperatures. Slow cooling through  $848^\circ\text{C}$  fractures the boule.

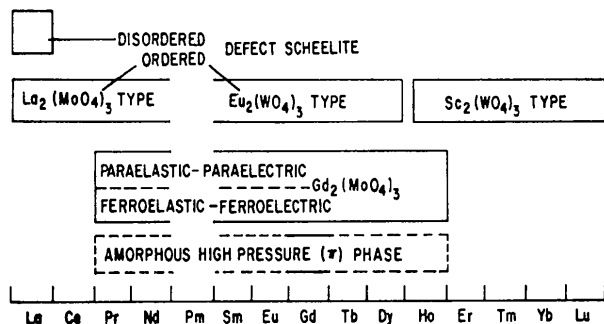


Fig. 1. Crystal structures of  $\text{L}_2(\text{MoO}_4)_3$  phases. Data for this figure were obtained through critical evaluation of the following reports: Nassau, Levinstein & Loiacono (1965); Abrahams & Bernstein (1966a); Borchardt & Bierstedt (1967); Jamieson, Abrahams & Bernstein (1969); Drobyshev Ponomarev, Folkina & Belov (1970); Nassau, Shiever & Keve (1971); Brixner, Bierstedt, Sleight & Licis (1971, 1972); Brixner, Sleight & Licis (1972); Nassau & Shiever (1972); Brixner (1972).

However, crystals large enough for X-ray work can be separated from the product and were kindly provided by L. H. Brixner. They are monoclinic, Laue symmetry  $2/m$ , and possible space groups  $Cc$  or  $C2/c$  of which  $Cc$  can be ruled out on the basis of the second-harmonic-generation test, as already reported by Brixner, Sleight & Licis (1972). These authors have also refined lattice constants for  $\text{La}_2(\text{MoO}_4)_3$ :  $a = 17.006$  (4),  $b = 11.952$  (3),  $c = 16.093$  (4) Å,  $\beta = 108.44$  (2) $^\circ$ ,  $V = 3102.8$  (1.3) Å $^3$ . Calculated and pycnometrically measured densities are  $4.865$  and  $4.75$  g cm $^{-3}$  respectively.

Crystals of the ordered  $\text{La}_2(\text{MoO}_4)_3$  structure are highly twinned. Single crystals can be found with polarized light. The crystal used for the structure determination was close in shape to a parallelepiped with dimensions  $105 \times 76 \times 15 \mu\text{m}$ . For the collection of the X-ray intensity data, an automated Picker single-crystal diffractometer was used with graphite monochromatized Mo  $K\alpha$  radiation, scintillation counter, and pulse-height discriminator. Scans were along  $2\theta$  with a speed of  $1.2^\circ 2\theta/\text{min}$  and a scan angle of  $2.2^\circ 2\theta$ . Background was counted for 20 sec at beginning and end of the scans. All reflections within the asymmetric quadrant of reciprocal space up to  $(\sin \theta)/\lambda = 0.62$  were recorded and corrected with the monochromator-modified Lorentz-polarization factor (Jeitschko, 1972). Absorption was accounted for according to Wuensch & Prewitt (1965), with the aid of a program written by Prewitt (1967). Transmission values varied between 32 and 85%.

### Structure determination and refinement

The resemblance of the  $\text{La}_2(\text{MoO}_4)_3$  powder pattern (Table 1) to that of scheelite was already recognized by Nassau, Levinstein & Loiacono (1965). The tetragonal scheelite subcell is also prominent on precession photographs. The relation of the tetragonal scheelite cell to that of  $\text{La}_2(\text{MoO}_4)_3$  is shown in Fig. 2. It can be seen that the  $\text{La}_2(\text{MoO}_4)_3$  cell comprises nine scheelite subcells. It was expected that the superstructure arises through the ordered arrangement of vacancies and La atoms on the Ca sites of the scheelite subcell. There are four such possibilities consistent with the space group  $C2/c$  of the  $\text{La}_2(\text{MoO}_4)_3$  superstructure. Intensity calculations for these arrangements (Yvon, Jeitschko & Parthé, 1969) readily revealed the ordered arrangement of the metal atoms. After least-squares refinement of the metal positions, oxygen positions were obtained from difference-Fourier syntheses calculated with a computer program by Fritchie & Guggenberger (1967).

The structure was refined with a full-matrix least-squares program by Finger (1969). Scattering factors for neutral atoms of Cromer & Mann (1968) were used, corrected for anomalous scattering (Cromer & Libermann, 1970). The function  $\sum w|KF_o - |F||^2$  was minimized where  $K$  is a scale factor and  $w$  the weight based on counting statistics. Reflections where  $F_o$  was less than three standard deviations were given zero weight

and are marked with an asterisk in the list of observed and calculated structure factors (Table 2). To account for secondary extinction, the relation  $I_{\text{corr}} = I_{\text{uncorr}} / (1 - cI_{\text{uncorr}})$  was used (Zachariasen, 1963), where  $c$  was  $0.4 \times 10^{-8}$ . The final refinements of the structure were done with anisotropic thermal parameters for the metal atoms and isotropic thermal parameters for oxygen atoms. The final conventional  $R$  value is 0.092 for a total of 3048 structure factors. For the 2031 structure factors greater than three standard deviations  $R$  is

Table 1. Evaluation of the first lines of a Guinier pattern of  $\text{La}_2(\text{MoO}_4)_3$ , Mo  $K\alpha$  radiation

hkl*	hk l	$d_c$	$d_o$	$I_c$	$I_o$	hkl*	hk l	$d_c$	$d_o$	$I_c$	$I_o$
11 0	9.6036	-	<1	-	-	000	60 0	2.6888	2.6885	19	8
11-1	8.9213	8.9251	9	w	-	20-6	2.6822	2.6816	19	8	
20 0	8.0664	-	<1	-	-	21 4	2.6626	-	<1	-	
00 2	7.6334	7.6398	5	vw	-	60-4	2.6237	-	<1	-	
11 1	7.5161	-	<1	-	-	42-5	2.6228	-	1	-	
20-2	6.7030	-	2	-	-	13 4	2.6192	-	1	-	
11-2	6.6129	6.6104	19	m	-	51 2	2.6180	-	<1	-	
02 0	5.9760	-	<1	-	-	51-5	2.6162	-	1	-	
02 1	5.5649	5.5629	18	s	-	31-6	2.5837	-	<1	-	
11 2	5.4931	-	<1	-	-	11-6	2.5829	-	<1	-	
31-1	5.2188	5.1764	2	vw	-	33-1	2.5776	-	1	-	
31 0	4.9031	-	<1	-	-	53-2	2.5774	-	<1	-	
11-3	4.8940	-	<1	-	-	4-3	2.5770	-	<1	-	
22-1	4.8494	-	1	-	-	04 3	2.5767	-	<1	-	
30 2	4.8334	4.8336	7	w	-	62-2	2.5594	-	<1	-	
31-2	4.8040	-	2	-	-	40-6	2.5453	-	<1	-	
22 0	4.8018	-	<1	-	-	00 6	2.5445	-	<1	-	
02 2	4.7055	-	3	-	-	24 2	2.5416	-	<1	-	
22-2	4.4606	-	<1	-	-	60-1	2.5384	2.5405	1	vw	
22 1	4.3520	4.3539	3	vw	-	62-3	2.5102	-	<1	-	
31 1	4.3303	4.3181	8	w	-	4-3	2.5085	-	<1	-	
31-3	4.1857	-	<1	-	-	53 9	2.5074	-	<1	-	
11 3	4.1826	-	<1	-	-	33-3	2.5067	-	<1	-	
10-2	4.1491	4.1479	3	vw	-	33 3	2.5054	-	<1	-	
40 0	4.0332	-	<1	-	-	13-5	2.4902	-	<1	-	
10-4	3.9694	-	1	-	-	73-5	2.4521	-	<1	-	
22-3	3.8757	-	<1	-	-	62 0	2.4520	2.4471	1	vw	
02 3	3.8745	-	<1	-	-	22-6	2.4470	-	1	-	
13 0	3.8678	-	<1	-	-	44-1	2.4434	-	<1	-	
13-1	3.8189	3.8158	1	vw	-	44-2	2.4347	-	1	-	
00 4	3.8167	-	<1	-	-	40 4	2.4167	-	<1	-	
11-4	3.8010	3.7986	6	w	-	62-4	2.4020	-	<1	-	
22 2	3.7591	-	<1	-	-	44 0	2.4009	-	<1	-	
13 1	3.6894	-	<1	-	-	24-4	2.3872	-	<1	-	
31 2	3.6723	-	<1	-	-	53 1	2.3824	2.3819	1	vw	
13-2	3.5668	3.5590	2	vw	-	22 5	2.3815	-	<1	-	
31-4	3.5487	-	<1	-	-	53-4	2.3814	-	1	-	
42-1	3.5468	-	<1	-	-	71-2	2.3805	-	1	-	
42-2	3.4082	-	<1	-	-	15 0	2.3646	-	<1	-	
40-4	3.3515	3.3511	3	vw	-	71-3	2.3574	-	1	-	
13 2	3.3493	-	1	-	-	31 3	2.3557	2.3542	1	vw	
42 0	3.3431	-	<1	-	-	31-6	2.3540	-	1	-	
11 4	3.3377	-	1	-	-	15-1	2.3533	-	1	-	
22-4	3.3064	-	<1	-	-	04 4	2.3528	-	1	-	
33-1	3.2587	3.2603	2	vw	-	11 6	2.3524	-	1	-	
51-1	3.2530	-	<1	-	-	44-3	2.3487	-	2	w	
51-2	3.2525	-	<1	-	-	24 3	2.3479	2.3481	2	w	
02 4	3.2166	-	<1	-	-	71-1	2.3468	-	<1	-	
112	42-3	3.2064	100	vvs	-	42-6	2.3422	-	<1	-	
22 3	3.2043	3.2059	99	vvs	-	02 6	2.3411	-	1	-	
103	33 0	3.2012	-	1	-	15 1	2.3405	-	<1	-	
13-3	3.1984	-	1	-	-	62 1	2.3186	2.3183	1	vw	
40 2	3.1752	-	<1	-	-	60 2	2.3160	-	<1	-	
33-2	3.1729	-	1	-	-	13 5	2.3128	-	1	-	
51 0	3.1151	-	<1	-	-	31 5	2.3102	-	1	-	
51-3	3.1137	-	<1	-	-	44 1	2.3061	-	<1	-	
31 3	3.1112	-	<1	-	-	15-2	2.2899	2.2891	1	vw	
42 1	3.1003	-	<1	-	-	71-4	2.2822	-	<1	-	
20 4	3.0925	-	1	-	-	71 0	2.2690	-	<1	-	
11-5	3.0822	-	<1	-	-	62-5	2.2557	-	<1	-	
33 1	3.0269	3.0207	3	vw	-	33 4	2.2527	-	<1	-	
51-5	3.0108	-	<1	-	-	31-7	2.2480	-	<1	-	
004	04 0	2.9880	2.9874	29	s	42 4	2.2404	-	<1	-	
33-3	2.9738	-	<1	-	-	60-6	2.2343	-	<1	-	
13 3	2.9726	-	<1	-	-	20 6	2.2324	-	<1	-	
04 1	2.9324	-	<1	-	-	44-4	2.2303	-	3	-	
42-4	2.9232	-	<1	-	-	15 2	2.2297	-	<1	-	
51 1	2.8845	2.8842	1	vw	-	53 2	2.2255	-	<1	-	
51-4	2.8828	-	<1	-	-	53-5	2.2244	-	1	-	
60-2	2.8323	-	2	-	-	11-7	2.2190	-	<1	-	
22-5	2.8290	-	2	-	-	33-6	2.2045	-	<1	-	
13-4	2.8260	2.8270	1	vw	-	13-6	2.2038	-	<1	-	
24-1	2.8113	-	<1	-	-	35-1	2.2023	-	1	-	
42 2	2.8040	-	<1	-	-	24-5	2.1876	-	<1	-	
24 0	2.8019	-	<1	-	-	35 0	2.1843	-	1	-	
04 2	2.7824	-	1	-	-	15-3	2.1834	-	<1	-	
33 2	2.7718	-	<1	-	-	44 2	2.1760	-	1	-	
11 5	2.7694	-	<1	-	-	35-2	2.1753	-	1	-	
22 4	2.7465	-	<1	-	-	71-5	2.1686	-	<1	-	
24-2	2.7291	-	<1	-	-	62 2	2.1602	-	1	-	
02 5	2.7190	-	<1	-	-	24 4	2.1488	-	2	-	
33-4	2.7175	-	<1	-	-	71 1	2.1440	2.1464	<1	vw	
24 1	2.7037	-	<1	-	-	22-7	2.1435	-	2	-	

\*Indices of scheelite-like subcell

0.055. Since this value depends mainly on the agreement of the scheelite-subcell reflections, it cannot be taken as an indicator for the accuracy of the whole structure. However, the value  $R=0.038$  for the 162 strongest subcell reflections is similar to the  $R$  value of 0.035 for the 916 superstructure reflections of the same intensity range. This indicates that the higher overall  $R$  value reported above is due to poor agreement in the large number of weak reflections because of poor counting statistics only. With the final parameters listed in Table 3 a difference-Fourier synthesis was calculated. None of the peaks in that synthesis was higher than one third the height of the oxygen peaks observed in previous syntheses for locating oxygen atoms. These residual peaks are all close to the positions of the metal atoms and probably result from small errors in absorption correction which were only in part compensated for by variations of anisotropic thermal-motion parameters. The positions of the metal vacancies corresponding to the voids in the scheelite subcell have also residual peaks of about one third the electron density of an oxygen atom. They do not necessarily indicate (slight) disorder, since an error in extinction correction in combination with an error in scale factor can account for them (these peaks were higher in previous difference-Fourier syntheses where some oxygen atoms had been placed incorrectly).

## Discussion

### Comparison of three defect scheelite structures

The  $\text{La}_2(\text{MoO}_4)_3$  structure is best described as a defect scheelite structure. The formula may be rewritten as  $\text{La}_{2/3}\square_{1/3}\text{MoO}_4$  where  $\square$  stands for the vacant sites. Ordered defect scheelite structures have been reported previously for  $\text{Eu}_2(\text{WO}_4)_3$  (Templeton & Zalkin, 1963) and  $\text{Bi}_2(\text{MoO}_4)_3$  (Cesari, Perego, Zazzetta,

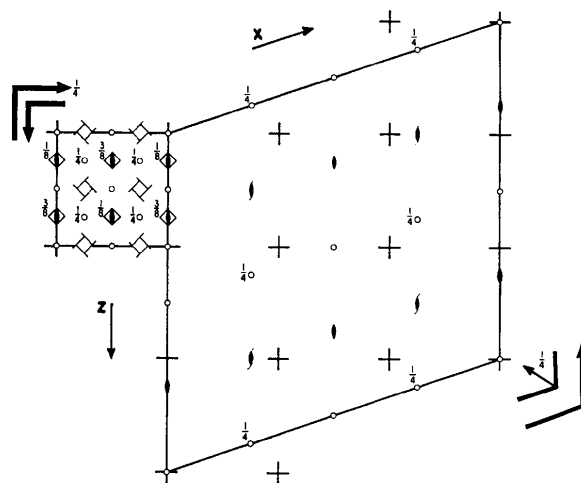


Fig. 2. Relation of the tetragonal scheelite subcell, space group  $I4_1/a$ , to that of the monoclinic  $\text{La}_2(\text{MoO}_4)_3$  superstructure cell, space group  $C2/c$ .



Table 3. *Positional and thermal parameters of  $\text{La}_2(\text{MoO}_4)_3$* 

Vibrational parameters ( $\times 10^5$ ) of La and Mo are defined through  $T = \exp(-\sum \sum h_i h_j \beta_{ij})$ . Isotropic thermal parameters  $B$  of oxygen atoms are given in  $\text{\AA}^2$ . Numbers in parentheses are e.s.d.'s in the least significant digits.

	$C2/c$	$x$	$y$	$z$	$\beta_{11}$	$\beta_{22}$	$\beta_{33}$	$\beta_{12}$	$\beta_{13}$	$\beta_{23}$
La(1)	8( <i>f</i> )	0.00680 (5)	0.62464 (8)	0.08908 (6)	127 (4)	138 (8)	102 (4)	10 (3)	63 (3)	-10 (4)
La(2)	8( <i>f</i> )	0.16545 (6)	0.12766 (7)	0.30250 (6)	136 (4)	124 (6)	94 (4)	4 (4)	62 (3)	-2 (4)
La(3)	8( <i>f</i> )	0.16552 (6)	0.87816 (7)	0.47751 (6)	127 (4)	109 (7)	98 (4)	5 (4)	58 (3)	10 (4)
Mo(1)	8( <i>f</i> )	0.00723 (8)	0.12871 (13)	0.42092 (9)	128 (7)	188 (13)	121 (7)	-7 (6)	76 (6)	-32 (6)
Mo(2)	8( <i>f</i> )	0.16659 (10)	0.63204 (12)	0.30928 (10)	118 (6)	256 (10)	98 (6)	-7 (7)	53 (5)	-20 (7)
Mo(3)	8( <i>f</i> )	0.17144 (9)	0.37590 (11)	0.13722 (10)	113 (6)	169 (10)	95 (6)	12 (6)	45 (5)	19 (6)
Mo(4)	8( <i>f</i> )	0.16166 (10)	0.38554 (11)	0.46572 (10)	130 (6)	164 (9)	117 (6)	30 (7)	61 (5)	-15 (6)
Mo(5)	4( <i>e</i> )	0	0.87311 (16)	$\frac{1}{4}$	114 (8)	125 (14)	83 (9)	0	32 (6)	0

Table 3 (*cont.*)

	$C2/c$	$x$	$y$	$z$	$B$
O(1)	8( <i>f</i> )	0.0719 (7)	0.0509 (9)	0.0547 (7)	1.31 (19)
O(2)	8( <i>f</i> )	0.4086 (6)	0.5484 (8)	0.0968 (6)	0.79 (17)
O(3)	8( <i>f</i> )	0.0444 (7)	0.1977 (9)	0.1774 (7)	1.15 (19)
O(4)	8( <i>f</i> )	0.4538 (6)	0.7225 (8)	0.9941 (7)	1.09 (18)
O(5)	8( <i>f</i> )	0.0872 (6)	0.5535 (9)	0.3293 (7)	1.28 (19)
O(6)	8( <i>f</i> )	0.2441 (7)	0.5554 (8)	0.2835 (7)	1.11 (18)
O(7)	8( <i>f</i> )	0.1155 (7)	0.7108 (9)	0.2163 (7)	1.49 (20)
O(8)	8( <i>f</i> )	0.2171 (7)	0.7162 (8)	0.4056 (7)	1.15 (18)
O(9)	8( <i>f</i> )	0.2068 (7)	0.2842 (8)	0.2245 (7)	1.20 (18)
O(10)	8( <i>f</i> )	0.1186 (7)	0.3030 (8)	0.0360 (7)	1.01 (18)
O(11)	8( <i>f</i> )	0.2575 (6)	0.4511 (8)	0.1240 (6)	0.81 (17)
O(12)	8( <i>f</i> )	0.0999 (7)	0.4676 (9)	0.1581 (7)	1.34 (19)
O(13)	8( <i>f</i> )	0.2132 (7)	0.6813 (9)	0.0652 (7)	1.66 (20)
O(14)	8( <i>f</i> )	0.1296 (7)	0.2878 (9)	0.3801 (7)	1.22 (19)
O(15)	8( <i>f</i> )	0.2347 (7)	0.4794 (9)	0.4470 (7)	1.43 (19)
O(16)	8( <i>f</i> )	0.0746 (6)	0.4571 (8)	0.4840 (6)	0.94 (18)
O(17)	8( <i>f</i> )	0.0482 (6)	0.7968 (8)	0.3507 (6)	0.52 (16)
O(18)	8( <i>f</i> )	0.0758 (7)	0.9609 (9)	0.2331 (7)	1.29 (19)

Manara & Notari, 1971). They are shown together with the  $\text{La}_2(\text{MoO}_4)_3$  structure in Fig. 3. The main differences between the structures are in the relative arrangements of the vacancies. There are of course many possible ordering schemes and it is not clear why for instance the unit cell adopted for  $\text{La}_2(\text{MoO}_4)_3$  is so large.

One way of analyzing differences among the three structures is by comparing distances between vacant sites. The shortest possible distances are the ones related by one  $4_1$  operation in the scheelite subcell. In the projections of Fig. 3 these sites are separated by one half translation period of the subcell. The separation in the projection direction is one quarter of the cell edge. Such sites are never both vacant in  $\text{La}_2(\text{MoO}_4)_3$  or  $\text{Eu}_2(\text{WO}_4)_3$ . Adjacent vacancies of that type do however occur in  $\text{Bi}_2(\text{MoO}_4)_3$ .<sup>\*</sup> As a consequence some of the oxygen atoms in  $\text{Bi}_2(\text{MoO}_4)_3$  have lost both of their A neighbors (as compared to a normal  $\text{ABO}_4$  scheelite). They are bonded only to one Mo atom at a distance of 1.65  $\text{\AA}$ , corresponding to a double bond (Cotton & Wing, 1965). Another type of interconnection of vacancies occurs whenever cations are missing on neighboring A sites with the same  $z$  coordinate. The distance

between the neighboring vacant sites corresponds to the length of the subcell  $a$  axis. As can be gathered by studying Fig. 3 three vacancies are connected in this manner in  $\text{La}_2(\text{MoO}_4)_3$ . Such connections do not occur in  $\text{Eu}_2(\text{WO}_4)_3$  or  $\text{Bi}_2(\text{MoO}_4)_3$ . With respect to the catalytic activity of  $\text{Bi}_2(\text{MoO}_4)_3$  (Adams & Jennings, 1963; Cesari *et al.*, 1971) it may be of interest, that neither one of these structures has vacancies connected continuously and therefore no obvious diffusion path is created through interconnection of vacant sites. However, the rapid transition of  $\text{La}_2(\text{MoO}_4)_3$  at 848  $^\circ\text{C}$  from a disordered to an ordered defect scheelite structure indicates that the La atoms are extremely mobile at the transition temperature and probably also at lower temperatures. The same may be assumed for Bi in  $\text{Bi}_2(\text{MoO}_4)_3$ . The catalytic activity of  $\text{Bi}_2(\text{MoO}_4)_3$  may also have to do with the Mo=O double bond mentioned above, which makes that oxygen suited as acceptor for radicals.

Atomic positions in  $\text{La}_2(\text{MoO}_4)_3$  deviate only little from those in scheelite. Considerable distortions from an ideal scheelite arrangement occur in both,  $\text{Bi}_2(\text{MoO}_4)_3$  and  $\text{Eu}_2(\text{WO}_4)_3$ . The distortions in  $\text{Bi}_2(\text{MoO}_4)_3$  may be attributed to the lone-pair effect of  $\text{Bi}^{3+}$ . In  $\text{Eu}_2(\text{WO}_4)_3$  the deviations from an ideal defect scheelite arrangement are due to the instability of the  $\text{WO}_4$  group: one of the two different W atoms in  $\text{Eu}_2(\text{WO}_4)_3$  has, besides four oxygen atoms at distances 1.72 to 1.81  $\text{\AA}$ , a fifth oxygen atom at 2.19  $\text{\AA}$ . For compositions which occur for both, molybdates and tungstates, it is sometimes observed that W is in octahedral and Mo in tetrahedral coordination. Examples are  $\text{ZnMoO}_4$  (Abrahams, 1967) and  $\text{ZnWO}_4$  (Sleight, 1972),  $\text{CdMoO}_4$  (Chichagov, Dem'yanets, Ilyukhin & Belov, 1967) and  $\text{CdWO}_4$  (Chichagov, Ilyukhin & Belov, 1966),  $\text{CuMoO}_4$  (Abrahams, Bernstein & Jamieson, 1968) and  $\text{CuWO}_4$  (Kihlberg & Gebert, 1970). Similarly W in  $\text{Eu}_2(\text{WO}_4)_3$  is compromising between tetrahedral and octahedral coordination while Mo in  $\text{La}_2(\text{MoO}_4)_3$  is stable in nearly perfect tetrahedral coordination.

#### *Interatomic distances and angles*

The  $\text{La}_2(\text{MoO}_4)_3$  structure has three independent La, five independent Mo, and eighteen independent oxygen atoms. Their near-neighbor environments are shown in Fig. 4 which was drawn with the aid of John-

<sup>\*</sup> The  $\text{Bi}_2(\text{MoO}_4)_3$  structure has been described in a short communication (Cesari *et al.*, 1971) and atomic positions have not been published. The present discussion is based on the drawing and the description given in that communication.

son's (1965) *ORTEP* program. Interatomic distances are listed in Table 4. The La atoms are eight-coordinated to oxygen as is also the case for the large cations in scheelite and the other defect scheelite structures. Although the lengths of the La–O distances generally reflect the differences in the coordination of the respective oxygen atoms, the *average* La–O distances are practically the same: 2.5198, 2.5202, and 2.5201 Å for La(1), La(2), and La(3) respectively. This is somewhat surprising since the ratio of two- and three-coordinated oxygen atoms is different for the three La atoms: La(3) has two, La(1) four, and La(2) six two-coordinated oxy-

gen atoms; the balance is always made up by three-coordinated oxygens.

Average oxygen distances from the two cation vacancies  $\square$  of the defect scheelite  $\text{La}_{2/3}\square_{1/3}\text{MoO}_4$  were also computed. They are, like the La atoms, in eight-fold oxygen 'coordination' with average distances 2.711 and 2.729 Å respectively. These distances are about 0.2 Å greater than the average La–O distances and are of course due to the electrostatic repulsion of the negatively charged oxygen atoms which are not counter-balanced by the missing La atom.

The oxygen environment of the five different Mo

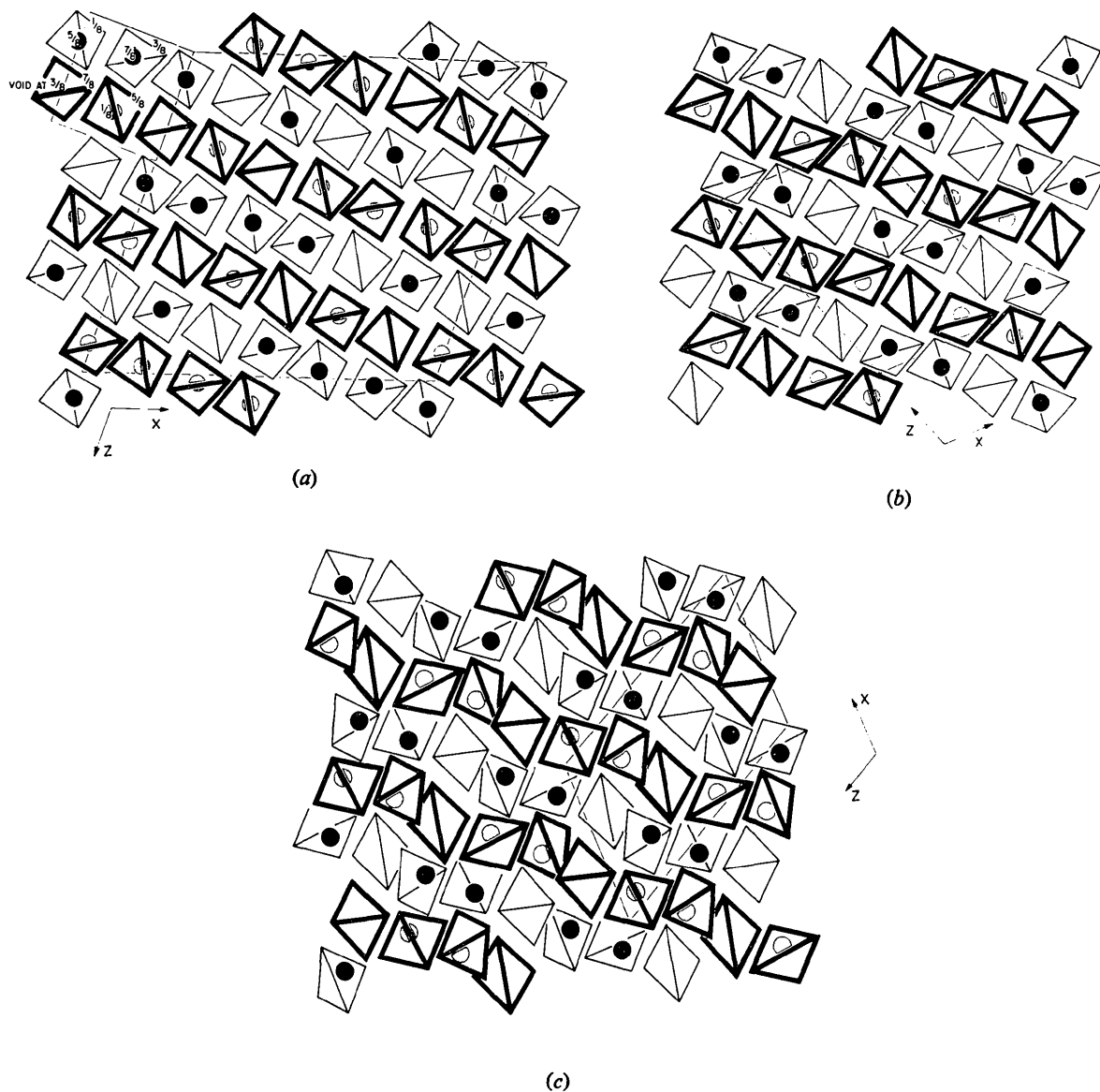


Fig. 3. Crystal structures of (a)  $\text{La}_2(\text{MoO}_4)_3$ , (b)  $\text{Eu}_2(\text{WO}_4)_3$ , and (c)  $\text{Bi}_2(\text{MoO}_4)_3$ . Projections are along the  $c$  axis of the scheelite subcell, which is outlined in the upper left-hand corner of the  $\text{La}_2(\text{MoO}_4)_3$  structure. Black dots and dotted circles represent La atoms above and below the  $\text{MoO}_4$  tetrahedra. The Mo atoms within the tetrahedra are not shown.

atoms in  $\text{La}_2(\text{MoO}_4)_3$  is almost perfectly tetrahedral with distances between 1.73 and 1.82 Å; the averages for each Mo atom vary between 1.771 and 1.781 Å. No other second-nearest oxygen is closer than 2.8 Å. Interatomic angles O–Mo–O are in between 104.0 and 116.5°.

Because of the vacancy formation, two thirds of the oxygen atoms are in only twofold coordination to cations as compared to the threefold coordination in scheelite. As expected (Shannon & Prewitt, 1969), these oxygen atoms are slightly closer to the cations than the three-coordinated ones. The differences in the

oxygen coordinations are also evident in thermal parameters: the average thermal parameter  $B$  (Table 3) for the twelve two-coordinated oxygen atoms is 1.30, while it is 0.87 for the six three-coordinated oxygen atoms. Interatomic metal–oxygen–metal angles for the twelve independent two-coordinated oxygen atoms vary from 124.6 to 148.1°. For the six oxygen atoms coordinated by three cations, Mo–O–La angles vary between 115.8 and 132.0° and La–O–La angles vary between 105.7 and 109.6°. These oxygen atoms are essentially coplanar with their three metal ligands. Nevertheless even their small deviations from the plane can

Table 4. *Interatomic distances (Å) in the structure of  $\text{La}_2(\text{MoO}_4)_3$*

All La–O distances shorter than 3.5 Å and all Mo–O distances shorter than 2.8 Å are listed. There are no O–O distances shorter than 2.75 Å. Standard deviations are all less than 0.013 Å.

La(1)	O(4)	2.479	Mo(1)	O(4)	1.730	O(2)	Mo(1)	1.820	O(11)	Mo(3)	1.786					
	O(12)	2.479		O(3)	1.754		La(3)	2.490		La(3)	2.548					
	O(7)	2.505		O(1)	1.778		La(2)	2.530		La(2)	2.568					
	O(16)	2.506		O(2)	1.820		O(3)	Mo(1)		1.754	O(12)	Mo(3)	1.748			
	O(5)	2.516		Mo(2)	O(7)			1.748		La(2)		2.524	La(1)	2.479		
	O(16)	2.525			O(5)			1.757		O(4)		Mo(1)	1.730	O(13)	Mo(4)	1.756
	O(17)	2.574			O(6)			1.760				La(1)	2.479		La(2)	2.534
O(10)	2.575	O(8)	1.819		O(5)	Mo(2)		1.757	O(14)	Mo(4)		1.756				
La(2)	O(14)	2.465	Mo(3)	O(9)		1.733	La(1)	2.516		La(2)	2.465					
	O(9)	2.475		O(12)		1.748	O(6)	Mo(2)		1.760	O(15)	Mo(4)	1.768			
	O(3)	2.524		O(11)	1.786	La(2)		2.524	La(3)	2.439						
	O(6)	2.524		O(10)	1.814	O(7)	Mo(2)	1.748	O(16)	Mo(4)	1.812					
	O(2)	2.530		Mo(4)	O(14)		1.756	La(1)		2.505	La(1)	2.506				
	O(13)	2.534			O(13)		1.756	O(8)		Mo(2)	1.819	O(17)	Mo(5)	1.814		
	O(18)	2.542			O(15)	1.768	La(3)		2.534	La(3)	2.552					
La(3)	O(11)	2.568	O(16)	1.812	O(8)	La(3)	2.549	O(9)	Mo(3)	1.733						
	La(3)	O(15)	2.439	Mo(5)		O(18)	1.749 (2×)		La(2)	2.475	O(18)	Mo(5)	1.749			
		O(1)	2.461			O(17)	1.814 (2×)		O(10)	Mo(3)		1.814	La(2)	2.542		
		O(2)	2.491		O(1)	Mo(1)	1.778	La(1)		2.575		La(3)	2.587			
		O(8)	2.534		La(3)	2.461										
		O(11)	2.548													
		O(8)	2.549													
O(17)		2.552														
O(10)	2.587															

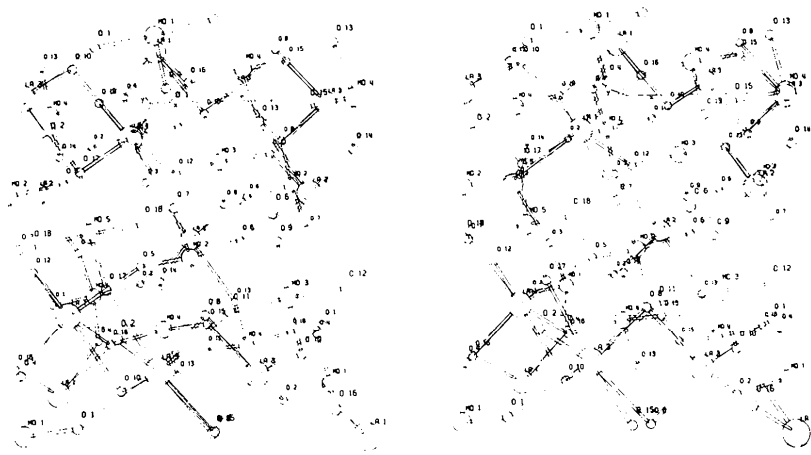


Fig. 4. Stereodiagram of near-neighbor environments in the  $\text{La}_2(\text{MoO}_4)_3$  structure. The asymmetric unit ( $\frac{1}{8}$  of the unit cell) in a view down the  $y$  axis is outlined.

be interpreted. If the plane is defined by the three metal ligands the central oxygen atom deviates from this plane by 0.098 Å for O(2), 0.268 Å for O(8), 0.096 Å for O(10), 0.043 Å for O(11), 0.066 Å for O(16) and 0.176 Å for O(17). The deviations occur always towards the second-nearest Mo atoms which are at distances of 2.92 to 3.23 Å. It is remarkable that the largest deviations of 0.268 and 0.176 Å occur for those oxygen atoms which have the closest Mo second-nearest neighbors at 2.92 and 3.04 Å respectively. The remaining four oxygen-Mo second-nearest neighbor distances range between 3.19 and 3.23 Å.

#### *Isostructural compounds*

As pointed out above, Brixner, Sleight & Licis (1972) have found the defect-scheelite molybdates of Ce, Pr, and Nd to be isostructural with  $\text{La}_2(\text{MoO}_4)_3$ . Weigel & Scherrer (1970) have reported  $\text{Pm}_2(\text{MoO}_4)_3$  to be isostructural with  $\text{Nd}_2(\text{MoO}_4)_3$  which they tentatively but erroneously indexed with a cell similar to  $\text{Eu}_2(\text{WO}_4)_3$ . The powder pattern reported by them for  $\text{Pm}(\text{MoO}_4)_3$  contains essentially only subcell reflections and it is therefore not possible to assign the correct superstructure -  $\text{La}_2(\text{MoO}_4)_3$  or  $\text{Eu}_2(\text{WO}_4)_3$  - to  $\text{Pm}_2(\text{MoO}_4)_3$ .

I am indebted to Dr L. H. Brixner for the well crystallized sample of  $\text{La}_2(\text{MoO}_4)_3$ . Mr D. M. Graham gave competent experimental help.

#### References

- ABRAHAMS, S. C. (1967). *J. Chem. Phys.* **46**, 2052-2063.  
 ABRAHAMS, S. C. & BERNSTEIN, J. L. (1966a). *J. Chem. Phys.* **45**, 2745-2752.  
 ABRAHAMS, S. C. & BERNSTEIN, J. L. (1966b). *Amer. Cryst. Assoc. Winter Meeting*, Abstract N1.  
 ABRAHAMS, S. C., BERNSTEIN, J. L. & JAMIESON, P. B. (1968). *J. Chem. Phys.* **48**, 2619-2629.  
 ADAMS, C. R. & JENNINGS, T. J. (1963). *J. Catalysis*, **2**, 63-68.  
 AIZU, K. (1969). *J. Phys. Soc. Japan*, **27**, 387-396.  
 BORCHARDT, H. J. & BIERSTEDT, P. E. (1966). *Appl. Phys. Lett.* **8**, 50-52.  
 BORCHARDT, H. J. & BIERSTEDT, P. E. (1967). *J. Appl. Phys.* **38**, 2057-2060.  
 BRIXNER, L. H. (1972). *Mater. Res. Bull.* **7**, 879-882.  
 BRIXNER, L. H., BIERSTEDT, P. E., SLEIGHT, A. W. & LICIS, M. S. (1971). *Mater. Res. Bull.* **6**, 545-554.  
 BRIXNER, L. H., BIERSTEDT, P. E., SLEIGHT, A. W. & LICIS, M. S. (1972). *Natl. Bur. Stand. Spec. Publ.* **364**, 437-443.  
 BRIXNER, L. H., SLEIGHT, A. W. & LICIS, M. S. (1972). *J. Solid State Chem.* **5**, 247-249.  
 BURBANK, R. D. (1965). *Acta Cryst.* **18**, 88-97.  
 CESARI, M., PEREGO, G., ZAZZETTA, A., MANARA, G. & NOTARI, B. (1971). *J. Inorg. Nucl. Chem.* **33**, 3595-3597.  
 CHICHAGOV, A. V., DEM'YANETS, L. N., ILYUKHIN, V. V. & BELOV, N. V. (1967). *Sov. Phys. Crystallogr.* **11**, 588-590.  
 CHICHAGOV, A. V., ILYUKHIN, V. V. & BELOV, N. V. (1966). *Sov. Phys. Crystallogr.* **11**, 11-13.  
 COTTON, F. A. & WING, R. M. (1965). *Inorg. Chem.* **4**, 867-873.  
 CROMER, D. T. & LIBERMAN, D. (1970). *J. Chem. Phys.* **53**, 1891-1898.  
 CROMER, D. T. & MANN, J. B. (1968). *Acta Cryst.* **A24**, 321-324.  
 DROBYSHEV, L. A., PONOMAREV, V. I., FROLKINA, I. T. & BELOV, N. V. (1970). *Sov. Phys. Crystallogr.* **15**, 391-394.  
 FINGER, L. W. (1969). Unpublished computer program for the least-squares refinement of crystal structures.  
 FRITCHIE, C. J. & GUGGENBERGER, L. J. (1967). Unpublished electron-density summation program.  
 JAMIESON, P. B., ABRAHAMS, S. C. & BERNSTEIN, J. L. (1969). *J. Chem. Phys.* **50**, 86-94.  
 JEITSCHKO, W. (1970). *Naturwissenschaften*, **57**, 544.  
 JEITSCHKO, W. (1972). *Acta Cryst.* **B28**, 60-76.  
 JOHNSON, C. K. (1965). *ORTEP*. Report ORNL-3794, Oak Ridge National Laboratory, Oak Ridge, Tennessee.  
 KAY, M. I., FRAZER, B. C. & ALMODOVAR, I. (1964). *J. Chem. Phys.* **40**, 504-506.  
 KEVE, E. T., ABRAHAMS, S. C. & BERNSTEIN, J. L. (1971). *J. Chem. Phys.* **54**, 3185-3194.  
 KIHLEBORG, L. & GEBERT, E. (1970). *Acta Cryst.* **B26**, 1020-1026.  
 NASSAU, K., LEVINSTEIN, H. J. & LOIACONO, G. M. (1965). *J. Phys. Chem. Solids*, **26**, 1805-1816.  
 NASSAU, K. & SHIEVER, J. W. (1972). *Natl. Bur. Stand. Spec. Publ.* **364**, 445-456.  
 NASSAU, K., SHIEVER, J. W. & KEVE, E. T. (1971). *J. Solid State Chem.* **3**, 411-419.  
 PREWITT, C. T. (1967). *ACACA*, an unpublished computer program for the absorption correction of single-crystal X-ray data.  
 SHANNON, R. D. & PREWITT, C. T. (1969). *Acta Cryst.* **B25**, 925-946.  
 SILLÉN, L. G. & NYLANDER, A. (1943). *Ark. Kem.* **17A** (4), 1-27.  
 SLEIGHT, A. W. (1972). *Acta Cryst.* **B28**, 2899-2902.  
 TEMPLETON, D. H. & ZALKIN, A. (1963). *Acta Cryst.* **16**, 762-766.  
 WEIGEL, F. & SCHERRER, V. (1970). *Radiochim. Acta*, **13**, 6-10.  
 WUENSCH, B. J. & PREWITT, C. T. (1965). *Z. Kristallogr.* **122**, 24-59.  
 YVON, K., JEITSCHKO, W. & PARTHÉ, E. (1969). A Fortran IV Program for the Intensity Calculation of Powder Patterns. Report of the Laboratory for Research on the Structure of Matter, Univ. Pennsylvania, Philadelphia, Pa.  
 ZACHARIASEN, W. H. (1963). *Acta Cryst.* **16**, 1139-1144.  
 ZALKIN, A. & TEMPLETON, D. H. (1964). *J. Chem. Phys.* **40**, 501-504.